Optical Properties of Spiroconjugated Charge-Transfer Dyes

Przemyslaw Maslak,*,† Anu Chopra,† Christopher R. Moylan,‡ Rüdiger Wortmann,§ Sonja Lebus,§ Arnold L. Rheingold,⊥ and Glenn P. A. Yap⊥

Contribution from the Department of Chemistry, The Pennsylvania State University, University Park, Pennsylvania 16802, IBM Almaden Research Center, 650 Harry Road, San Jose, California 95120, Institut für Physikalische Chemie, Johannes Gutenberg-Universität, Jakob Welder-Weg 11, 55099 Mainz, Germany, and Department of Chemistry, University of Delaware, Newark, Delaware 19716

Received September 27, 1995⊗

Abstract: A new type of intramolecular charge-transfer dye has been prepared. The LUMO of the acceptor part (1,3-indandione) in these compounds is spiroconjugated with the HOMO of the donor part (aromatic diamine or amino thiol). The interaction between the donor and acceptor is controlled by the energy and symmetry of the frontier orbitals. The ground state dipole moments of these compounds are aligned along the long molecular axes. In the solid state, distortions of structures are observed that are consistent with partial electron shift from the donor to the acceptor. Much more pronounced electron density shifts accompany the electronic transition that is observed in the visible region of the spectrum. These transitions are of the charge-transfer (CT) type, as shown by solvatochromic and electrooptical studies. The excited state dipole moments are in the direction opposite to that of the ground state. These observations are consistent with the excited state having radical ion pair character. The new dyes are modeled using a simple Mulliken charge-transfer theory. The mixing coefficient of neutral and ionic wave functions describing these systems is used as a measure of spiroconjugation between the subchromophores. The electrooptical data provide an estimate of the contribution of the CT transitions to the hyperpolarizabilities (β) within the two-state model. The measured values of β indicate, however, that spiro dyes have two opposing contributions to their hyperpolarizabilities, one from the CT transition and one due to the acceptor subchromophore.

Introduction

Charge-transfer (CT) interactions play an important role in the area of organic materials with unusual electric, magnetic, or optical properties.[1−3] The donor and acceptor components of such materials have been largely limited to planar conjugated π-systems. As a consequence, the materials obtained are quasi-one-dimensional. We have initiated a project to explore charge-transfer interactions in systems with increased dimensionality.[4,5] Our design is based on spiroconjugation,[6,7] an interaction that allows for electronic coupling between two mutually perpendicular π-subsystems.

In a general case, two π-networks (A and D) are joined by a spiro atom (Chart 1). Only the molecular orbitals of the two π-subsystems that have the same symmetry may interact, leading to molecular orbitals spanning the entire system. In an idealized reference frame, the crucial symmetry elements are the two perpendicular bisecting planes (Chart 1). As shown in the Fischer projection of the four atomic orbitals on atoms directly attached to the spiro atom, only those orbitals of the subsystems that are antisymmetric with respect to the two planes lead to a nonzero overlap required for intramolecular interactions.

Chart 1

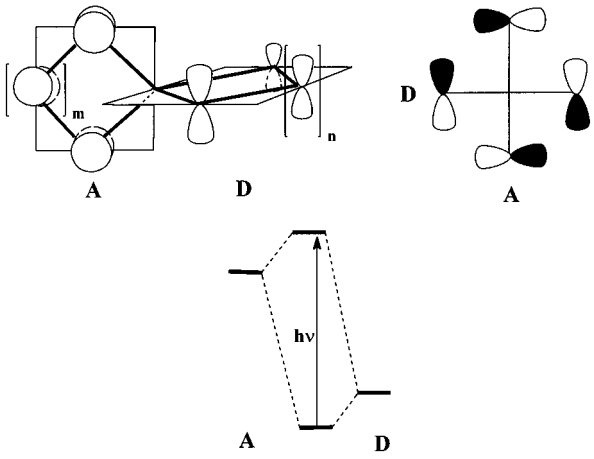

The main contribution to charge-transfer interactions is provided by the frontier orbitals. Thus, in our design the HOMOs and LUMOs of the π-subsystems should satisfy the

† The Pennsylvania State University.
‡ IBM Almaden Research Center.
§ Johannes Gutenberg-Universität.
⊥ University of Delaware.
⊗ Abstract published in *Advance ACS Abstracts,* January 15, 1996.

(1) (a) Carter, F. L., Ed. *Molecular Electronic Devices*; Marcel Dekker: New York, 1982; Vol. I; 1987; Vol. II. (b) Wudl, F. *Acc. Chem. Res.* **1984**, *17*, 227. (c) Wudl, F. In *The Physics and Chemistry of Low Dimensional Solids*; Alcacer, L., Ed.; D. Reidel Publishing Co.: Dordrecht, The Netherlands, 1980; p 265. (d) Cowan, D. O.; Wiyguli, F. M. *Chem. Eng. News* **1986**, *64*, 28. (e) Miller, J. S.; Epstein, A. J. *Angew. Chem., Int. Ed. Engl.* **1987**, *26*. 287. (f) Torrance, J. B. *Mol. Cryst. Liq. Cryst.* **1985**, *126*, 55. (g) Bechgaard, K.; Jérome, D. *Sci. Am.* **1982**, 52. (h) Gompper, R.; Wagner, H.-U. *Angew. Chem., Int. Ed. Engl.* **1988**, 27, 1437. (i) Bloor, D. *Mol. Cryst. Liq. Cryst.* **1993**, *234*, 1. (j) Aviram A. *Mol. Cryst. Liq. Cryst.* **1993**, *234*, 13.

(2) (a) Miller, J. S.; Epstein, A. J.; Reiff, W. M. *Chem. Rev.* **1988**, *88*, 201. (b) Miller, J. S.; Epstein, A. J.; Reiff, W. M. *Acc. Chem. Res.* **1988**, *21*, 114. (c) Miller, J. S.; Epstein, A. J. *Mol. Cryst. Liq. Cryst.* **1993**, *234*, 133. (d) Dougherty, D. A *Acc. Chem. Res.* **1991**, *24*, 88. (e) Iwamura, H.; Koga, N. *Acc. Chem. Res.* **1993**, *26*, 346. (f) Rajca, A. *Chem Rev.* **1994**, *94*, 871.

(3) (a) Prasad, P. N.; Williams, D. J. *Introduction to Nonlinear Optical Effects in Molecules and Polymers*; Wiley-Interscience: New York, 1991. (b) Khanarian, G., Ed. *Molecular and Optoelectronic Materials: Fundamentals and Applications*; SPIE: San Diego, 1986. (c) Eaton, D. F. *Science* **1991**, *253*, 281. (d) Glass, A. M. *Science* **1987**, *235*, 1003. (e) Williams D. J. *Angew. Chem., Int. Ed. Engl.* **1984**, *23*, 690. (f) Chemla, D. S., Zyss, J., Eds. *Nonlinear Optical Properties of Organic Molecules and Crystals*; Academic Press: New York, 1987; Vols. 1 and 2. (g) Lyons, M. H., Ed. *Materials for Nonlinear and Electro-optics*; Institute of Physics Conference Series Number 103; Institute of Physics: Bristol, New York, Cambridge, 1989. (h) Prasad, P. N.; Reinhardt, B. A. *Chem. Mater*. **1990**, *2*, 660. (i) Eaton, D. F. *CHEMTECH* **1992**, 308. (j) Marder, S. R. In *Materials Chemistry: An Emerging Discipline*; Interrante, L. V., Casper, L. A., Ellis, A. B., Eds.; American Chemical Society: Washington, DC, 1995; p 189.

0002-7863/96/1518-1471$12.00/0

symmetry requirements. Specifically, for optical applications[3] we have selected acceptors (A) that have antisymmetric LUMOs and donors (D) that possess antisymmetric HOMOs. The interactions between these orbitals of the two subsystems give rise to two new spiroconjugated orbitals spanning the entire molecule. The lower-energy one, the new HOMO, corresponds to the bonding combination of the subsystem orbitals, and the higher-energy antibonding combination becomes a new LUMO. This mixing of spiroconjugated subsystem orbitals results in a HOMO that has some electron density on the acceptor part, and a LUMO that has nonzero orbital coefficients on the donor part. The electronic transition between these frontier orbitals is formally allowed, and should correspond to a charge-transfer transition[8] (Chart 1).

In practice, the strict symmetry requirements may be relaxed.[9] As long as the coefficients of the frontier orbitals change signs versus the bisecting planes, the overlap depicted in Chart 1 will provide for the mechanism of coupling between the two subsystems. Thus, a variety of substitution patterns are possible, increasing flexibility in the design of these spiroconjugated dyes.[5]

In the spiro dyes presented here the role of the acceptor is played by the 1,3-indandione moiety.[10,11] This π-subsystem has an antisymmetric LUMO.[12] The donor parts are based on aromatic diamines or amino thiols.[13] The HOMO symmetry in these donors depends on the selection of the aromatic residue.[12] The 1,2-phenyl derivatives possess symmetrical HOMOs and, therefore, are not expected to spiroconjugate with the acceptor's LUMO. The 1,8-naphthyl and 2,2′-biphenyl subsystems, on the other hand, offer antisymmetric[12] HOMOs that have the potential to spiroconjugate with the indandione's LUMO. The new dyes can be easily constructed by a simple condensation reaction between the ninhydrin (or its derivatives) and the corresponding *N*-methylated diamines or amino thiols.

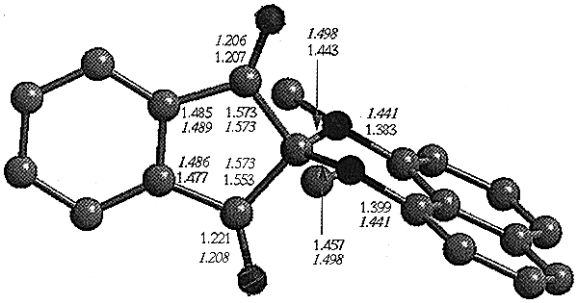

Figure 1. X-ray structure of **2**. Selected bond lengths (Å) illustrating the distortions in the structure are shown in normal typeface. The calculated bond lengths (PM3) are shown in italics. Hydrogen atoms have been omitted for clarity. The estimated standard deviations for the indicated bonds are in the 0.005−0.008 Å range.

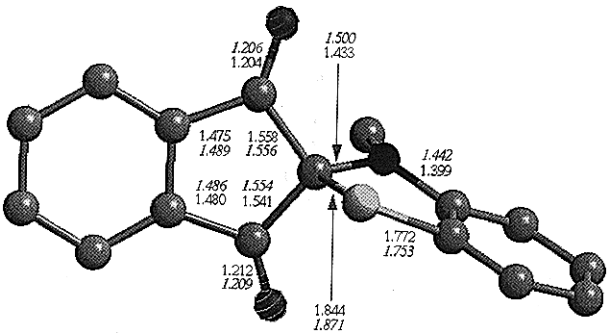

Figure 2. X-ray structure of **4**. Legend is as in Figure 1.

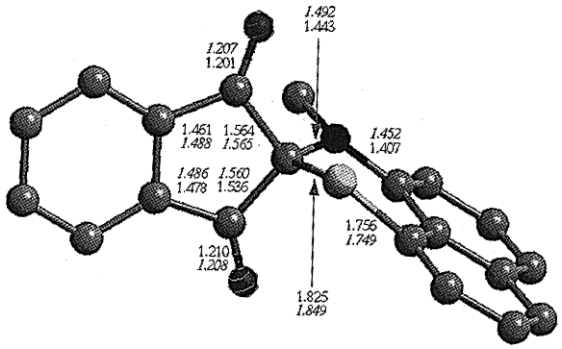

Figure 3. X-ray structure of **5**. Legend is as in Figure 1.

Results and Discussion

The spiro compounds **1**−**6** were obtained by an acid-catalyzed condensation of ninhydrin (or 5,6-dimethoxyninhydrin in the case of **6**) with the *N*-methylated diamines or amino thiols with azeotropic removal of water. All the desired products were highly colored, and were easily separated from side products. Four of the compounds gave single crystals suitable for X-ray analysis[14] (Figures 1−4).

The X-ray crystal structures have significantly lower symmetry than one would predict on the basis of simple geometrical arguments. Not only are nitrogen atoms pyramidalized (as expected), but the whole donor moiety is slightly twisted sideways from the acceptor plane. The lengths of "symmetrically" disposed bonds are not equal. The bond distortions can be accounted for by an electron density shift from the amine donor to the indandione acceptor as shown in Scheme 1. For example, in chromophore **2** (which illustrates the general trend)

(4) Maslak, P. *Adv. Mater*. **1994**, *6*, 405. (b) Maslak, P.; Augustine, M. P.; Burkey, J. D. *J. Am. Chem. Soc*. **1990**, *112*, 5359. Compare also the following: (c) Tour, J. M.; Wu, R.; Schumm, J. S. *J. Am. Chem. Soc*. **1990**, *112*, 6662; **1991**, *113*, 7064. (d) Aviram, A. *Mol. Cryst. Liq. Cryst.* **1993**, *234*, 13. (e) Hush, N. S.; Wong, A. T.; Bacskay, G. B.; Reimers, J. R. *J. Am. Chem. Soc.* **1990**, *112*, 4192.

(5) Maslak, P.; Chopra, A. *J. Am. Chem. Soc.* **1993**, *115*, 9332.

(6) (a) Simmons, H. E.; Fukunaga, T. *J. Am. Chem. Soc*. **1967**, *89*, 5208. (b) Hoffmann, R. Imamura, A.; Zeiss, G. D. *J. Am. Chem. Soc*. **1967**, *89*, 5215.

(7) For a review see: Durr, H.; Gleiter, R. *Angew. Chem., Int. Ed. Engl.* **1978**, *17*, 559.

(8) (a) Mulliken, R. S.; Pearson, W. B. *Molecular Complexes: A Lecture and Reprint Volume*; Wiley-Interscience: New York, 1969. (b) Foster, R. *Organic Charge-Transfer Complexes*; Academic Press: New York, 1969. (c) Nagakura, S. *Excited States*; Academic Press: New York, 1975; Vol. 2, p 321.

(9) The symmetry is used here in a conceptual (i.e., approximate) way, and does not strictly reflect the symmetry of the components or spiro compounds.

(10) Ethylenediamine analogs of spiro dyes have been prepared: (a) Schönberg, A.; Singer, E.; Osch, M.; Hoyer, G.-A. *Tetrahedron Lett*. **1975**, 3217. (b) Schönberg, A.; Singer, E.; Eschenhof, B.; Hoyer, G.-A. *Chem. Ber*. **1978**, *111*, 3058. (c) Schönberg, A.; Singer, E. *Tetrahedron* **1978**, *34*, 1285. (d) Schönberg, A.; Singer, E.; Eckert, P. *Chem. Ber*. **1980**, *113*, 3094. (e) Sheldrick, W. S.; Schönberg, A.; Singer, E. *Acta Crystallogr*. **1982**, *B38*, 1355.

(11) Spiro donor−acceptors with oxygen and sulfur atoms on the donor moiety have recently been reported: Gleiter, R.; Hoffmann, H.; Irngartinger, H.; Nixdorf, M. *Chem. Ber*. **1994**, *127*, 2215.

(12) The symmetry of the subchromophores (ref 9) was established using the semiempirical MNDO-PM3 calculations (ref 15) using Spartan 3.1 (Wavefunction Inc.).

(13) Compare the following: (a) Gleiter, R.; Uschmann; J. *J. Org. Chem*. **1986**, *51*, 370. (b) Gleiter, R.; Haider R.; Quast, H. *J. Chem Res., Synop.* **1978**, 138. (c) Spanget-Larsen, J.; Uschmann, J.; Gleiter, R. *J. Phys. Chem.* **1990**, *94*, 2334.

(14) Further details of X-ray structures, including crystal packing arrangements, will be discussed elsewhere.

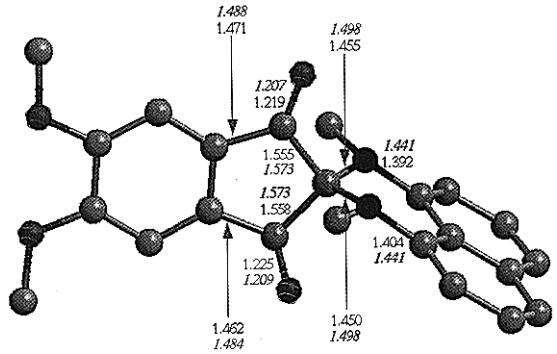

Figure 4. X-ray structure of **6**. Legend is as in Figure 1.

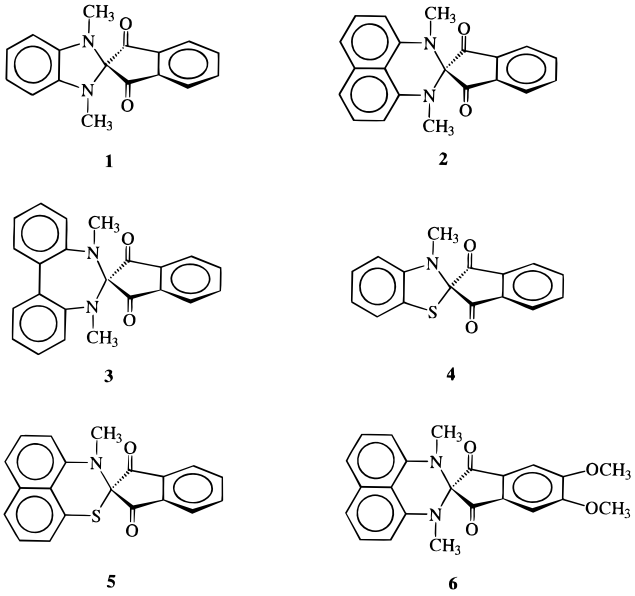

one of the nitrogens serves as the electron source. It becomes less pyramidal than the other, and its bond with the spiro carbon is shorter than that of the other nitrogen. In turn, the bond between one of the carbonyl carbons and the spiro carbon becomes longer than the corresponding bond of the other carbonyl carbon. Ultimately, this second carbonyl group becomes the acceptor of electron density, the C−O bond lengthens, and the carbonyl carbon pyramidalizes slightly.

The origin of these distortions can be traced to the pyramidalization of the nitrogen atoms. In the solid state the nitrogen inversion (requiring movement of the aryl moieties) is blocked. The *N*-aryl moiety is bent toward one of the carbonyl groups, and the nitrogen lone pairs point up (Scheme 1). As the result of increased orbital overlap with one of these lone pairs, the *upper* carbonyl carbon−spiro carbon bond is elongated. The nitrogen serving as the donor forms a shorter bond with the spiro carbon than the other nitrogen, thus twisting the donor moiety away from the acceptor plane. According to the electron flow (Scheme 1), the lower carbonyl serves as the acceptor, and the *N*-aryl moiety is always bent toward it.

These bond distortions result in chiral structures. Indeed the crystal unit cells contain both enantiomers[14] that correspond to the selection of one or the other nitrogen as the donor atom. The stereoelectronic factors associated with the electron density shift are rather poor (the two π-systems are nearly perpendicular) and the distortions are quite small (sometimes within the estimated standard deviations), but consistent for all the compounds examined. On the basis of the bond lengths, in **4** and **5** (Figures 2 and 3) apparently only the nitrogen atom serves

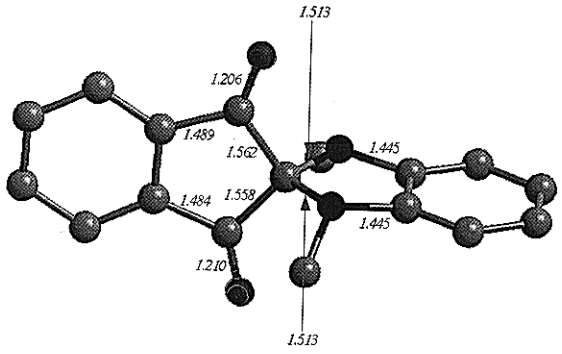

Figure 5. Calculated (PM3) structure of **1**. Selected bond lengths (Å) are shown in italics. Hydrogen atoms have been omitted for clarity.

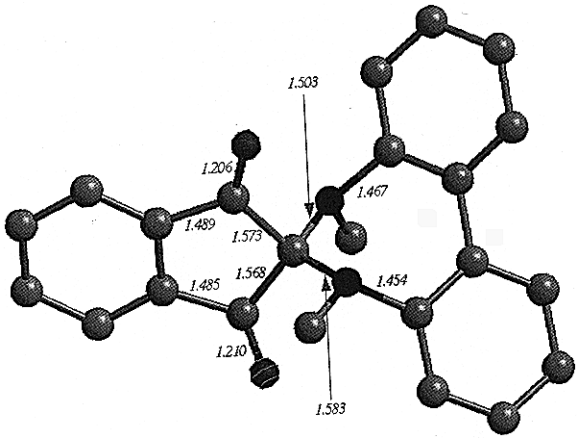

Figure 6. Calculated (PM3) structure of **3**. Legend is as in Figure 5.

Scheme 1

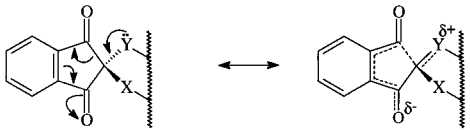

as the donor (rather than sulfur), and in **6** (Figure 4) the distortions are smaller than in other compounds, as expected on the basis of the diminished electron demand of the carbonyls due to the presence of the methoxy groups on the acceptor moiety.

The semiempirical calculations[15] (PM3) yield structures that are almost devoid of these distortions. The small differences in calculated bond lengths (on the order of thousandths of an angstrom) do nevertheless follow the trend observed in solid state structures. Crystal packing[14] (intermolecular interactions) might be responsible for accentuating the diminished symmetry. In general, the calculated and observed bond lengths and angles are comparable, and it can be assumed that the calculated structures for **1** and **3** represent the shapes of these molecules quite well (Figures 5 and 6).

In solution the nitrogen inversion is rapid on the ^{1}H and ^{13}C NMR time scale. The distortions associated with the inversion should average out under these conditions. Indeed, only one set of signals consistent with the presence of symmetry planes for the acceptor and the donor (where appropriate) is observed for the spiro compounds. Even at −70 °C there is no evidence of any signal broadening.

All spiro dyes showed an absorption band in the visible region (Figures 7−11). No such bands would be expected from the

(15) Stewart, J. J. P. J. *Comput.-Aided Mol. Des.* **1990**, *4*, 1.

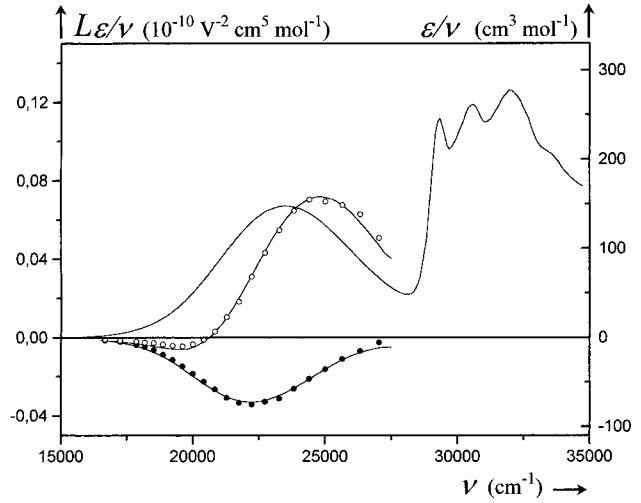

Figure 7. Absorption (ϵ/ν) and electrooptical absorption ($L\epsilon/\nu$) spectra of **2** in 1,4-dioxane. Experimental data points for parallel (hollow circles) and perpendicular (filled circles) polarization of the incident light relative to the applied electric field are connected by lines obtained from regression analysis.

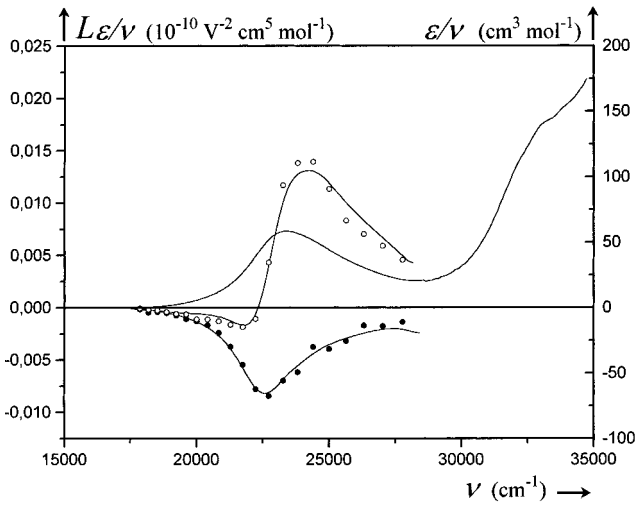

Figure 8. Absorption (ϵ/ν) and electrooptical absorption ($L\epsilon/\nu$) spectra of **3** in 1,4-dioxane. Legend is as in Figure 7.

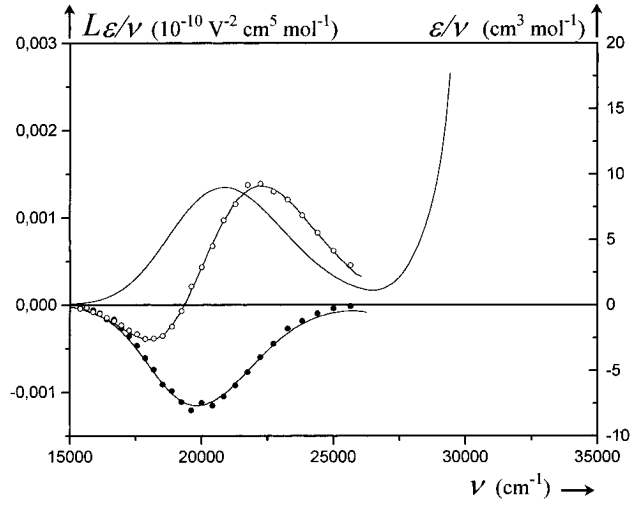

Figure 9. Absorption (ϵ/ν) and electrooptical absorption ($L\epsilon/\nu$) spectra of **4** in 1,4-dioxane. Legend is as in Figure 7.

presence of either of the two subchromophores, since both the electron acceptors (indan-1,3-diones) and the electron donors (such as diaminobenzene or diaminonaphthalene) have no

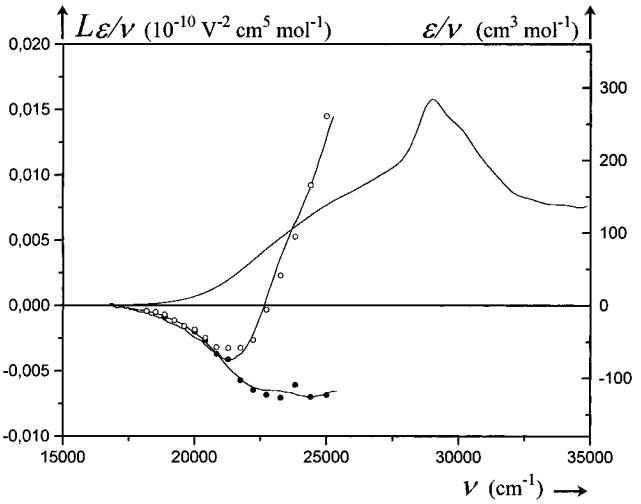

Figure 10. Absorption (ϵ/ν) and electrooptical absorption ($L\epsilon/\nu$) spectra of **5** in 1,4-dioxane. Legend is as in Figure 7.

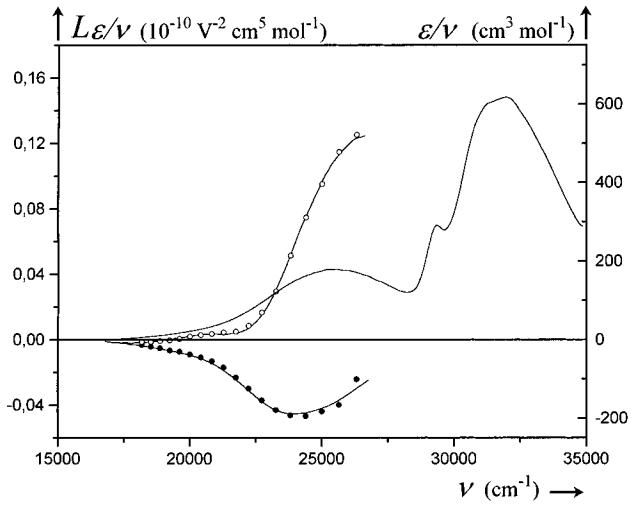

Figure 11. Absorption (ϵ/ν) and electrooptical absorption ($L\epsilon/\nu$) spectra of **6** in 1,4-dioxane. Legend is as in Figure 7.

significant absorbance above 370 nm. The intramolecular nature of the charge-transfer transition was confirmed using model donor and acceptor compounds. Concentrated solutions of 1,4-diethyl-1,2,3,4-tetrahydroquinoxaline and 2,2-dimethylindan-1,3-dione in methylene chloride, as well as neat mixtures of these model compounds, did not show any absorption bands in the visible region. Similarly, no visible absorptions were detected for 2,2-dichloroindan-1,3-dione, 1,2,2,3-tetramethylperimidine, or their mixture in methylene chloride.

In contrast, **1** and **2** have pronounced absorptions bands in the visible region (λ_{max} = 552 and 414 nm, respectively, in methylene chloride). Apparently in the model systems the orbital overlap is too small, or the HOMO−LUMO energy gap is too large. For **1** and **2** the intensity of the charge-transfer bands followed the Beer−Lambert law over more than a 1000-fold change in concentration, confirming the intramolecular nature of the transition. The fact that both the extinction coefficients and λ_{max} values remained constant over the dilution range (5×10^{-6} to 5×10^{-3} M) also excludes complexation between the dye molecules.

In **1** and **4** the symmetry of the donor is mismatched with that of the acceptor. The interaction between the components is weak, and mainly of inductive nature. As a result, the HOMO−LUMO transition is *forbidden*. The observed charge-transfer bands clearly show low probability of these transitions (ϵ_{536} = 140 M^{-1} cm^{-1} for **1** and ϵ_{464} = 170 M^{-1} cm^{-1} for **4** in

Table 1. Optical Properties[a] of Spiro Dyes

	1	**2**	**3**	**4**	**5**	**6**
λ_{max}[b] (nm)	560	421	427	427	390	391
σ[c] ($\times 10^{-3}$ cm^{-1})	5.88	6.53	4.91	5.91		6.69
μ_g[d] (D)	0.6	2.9	1.7	0.7	2.9	3.3
μ_g[e] (D)		4.8(1)	3.5(1)	3.2(1)	2.3(2)	5.4(1)
μ_g[f] (D)		4.65(4)	3.4(1)	3.1(1)	2.7(1)	4.2(1)
μ_g[g] (D)	3.20	4.09	2.05	2.68	2.98	3.66
μ_e[e] (D)		−5.6(5)	−1.9(7)	−2.6(2)	−8(2)	−5.8(7)
μ_e[h] (D)	−4(1)	−5.6	−4.2(1)	−3.7(1)		−5.7(1)
$\Delta\mu$[i] (D)	−7(1)[h]	−10.4(5)	−5.4(6)	−5.8(2)	−10(2)	−11.2(6)
Δ[j] (D)	7.5(9)	11.9(4)	6.4(5)	5.9(2)	12(1)	13.0(5)
c[j]	0.08(8)	0.26(1)	0.29(3)	0.11(1)	0.26(4)	0.27(1)
β[k] (1.907 μm)		<2.0	4.4(8)	8(1)	2(2)	23(6)
β(CT)[l]	−0.2(1)	−15.5(8)	−3.7(8)	−0.62(8)	−13(2)	−17.5(8)
$\Delta\beta$[m]		17.5	8.1	9.1	15.6	39.5

[a] The estimated errors are shown in parentheses as standard deviations of the least significant digits. [b] In 1,4-dioxane. [c] Widths of CT bands at half-height in acetonitrile. [d] From eq 4, in 1,4-dioxane (1 D = 3.336×10^{-30} C m). [e] From EOAM in 1,4-dioxane. [f] From the Guggenheim expression (ref 23), in chloroform. [g] Calculated (PM3). [h] From solvatochromic studies. The dipole of **2** was scaled to the EOAM result (see text). [i] $\Delta\mu = \mu_e - \mu_g$. [j] From the Mulliken model (eqs 5−10). [k] EFISH measurements in chloroform. All β values are $\times 10^{30}$ esu (10^{-30} esu = 0.3711×10^{-50} C m^3 V^{-2}). [l] Calculated from eq 11. [m] The difference between the observed and calculated β values, $\Delta\beta = \beta - \beta$(CT).

acetonitrile). The transitions occur most likely due to symmetry breaking analogous to that observed in the solid state structures (see above). The difference in the position of the charge-transfer bands is directly related to the donor strength. As judged by the oxidation potentials of **1** (E^{ox} = 0.48 V vs SCE) and **4** (E^{ox} = 0.95 V) the diamino compound has significantly higher HOMO energy than the amino thiol derivative.

In contrast, the naphthyl-based donors in **2**, **5**, and **6** have an antisymmetric HOMO (vs the plane of the dione). These orbitals spiroconjugate with the LUMO of the acceptor part. As a result of this orbital mixing, the CT transition is *allowed* ($\epsilon \geq 3800$ M^{-1} cm^{-1} for all these compounds). In all the cases the absorption band is significantly shifted to higher energies (when compared to **1** or **4)**, reflecting both the differences in the donor or acceptor strengths and the effects of spiroconjugation.[5]

In **3**, the HOMO of the donor has correct symmetry, but it is of lower energy than that in **2** (E^{ox} = 1.21 V for **3**, E^{ox} = 0.72 V for **2**). Additionally, the seven-membered ring formed may not allow for optimum overlap between the nitrogen orbitals and the corresponding carbonyl carbon orbitals (Figure 6). As a result, the probability of transition is diminished ($\epsilon_{428} = 1.35 \times 10^3$ M^{-1} cm^{-1}).

In all these spiro compounds, the fluorescence intensity was extremely low, only slightly higher than the background. Variations in the excitation wavelengths (from UV to visible) or polarity of the solvent (acetonitrile, dichloromethane, benzene, formamide, dimethyl sulfoxide, and hexane) did not affect the results. The shape of very weak emission bands was similar to the shape of the charge-transfer absorption bands, and the emission occurred at a longer wavelength, as expected.

The charge-transfer bands of the dyes showed pronounced negative solvatochromism;[16] i.e., a hypsochromic shift of the charge-transfer band occurred on increasing the solvent polarity. Following the McRae formalism,[17] the expression for the solvatochromic shifts in absorption frequency of a molecule can be written as

$$\omega_{solvent} - \omega_{vacuum} = A\left[\frac{n^2-1}{2n^2+1}\right] + B\left[\frac{\epsilon-1}{\epsilon+2} - \frac{n^2-1}{n^2+2}\right] \quad (1)$$

$$B = \frac{2}{4\epsilon_0 \pi \hbar a^3}\mu_g(\mu_g - \mu_e \cos\Phi) \quad (2)$$

where $\omega_{solvent}$ is the frequency of transition (s^{-1}) in a solvent, ω_{vacuum} is the frequency of transition in a vacuum, n is the refractive index of the solvent, ϵ is the dielectric constant of the solvent, ϵ_0 is the permeability of the vacuum, A and B are constants characteristic of the molecule, μ_g is the dipole moment of the ground state of the molecule, μ_e is the dipole moment of the excited state of the molecule, Φ is the angle between the direction of μ_g and the direction of μ_e, and a is the solvent cavity radius. This last quantity is not well defined, and different approaches to its estimation can be found in the literature.[18] As in a previous paper,[19] we avoid any arbitrariness in choosing this parameter by scaling the solvatochromic results for μ_e to the results of electrooptical absorption measurements (EOAM), which are more accurate in general. Compound **2** was selected as a typical representative of the present class of chromophores. Agreement of solvatochromic and EOAM results was obtained by setting a equal to $0.71L/2$ (where L is the diameter of the smallest sphere enclosing the molecule). This choice of the cavity radius was then equally applied to the other spiro CT dyes.

A linear regression of the solvatochromic data yields B values for the dyes (see the Experimental Section). Using measured values of the ground state dipole moments (from electrooptical studies, or from calculations in the case of **1**) and geometrical data from X-ray structures (or calculated structures in the case of **1** and **3**), and assuming in all cases that $\Phi = 180°$ (see below), excited state dipole moments were estimated for the compounds (Table 1). The values are in reasonably good agreement with the values obtained from electrooptical experiments.

In electrooptical absorption (EOA) experiments the effect of an external electric field (E_0) on the absorption of linearly polarized light by a dilute solution of an organic compound is given by[20]

$$L\epsilon/\nu = \frac{(\epsilon^E/\nu) - (\epsilon/\nu)}{{E_0}^2} \quad (3)$$

where $\epsilon = \epsilon(\nu)$ and $\epsilon^E = \epsilon(\varphi,\nu)$ represent the molar extinction coefficients in the absence and presence of the applied electric

(16) Reichardt, C. *Solvents and Solvent Effects in Organic Chemistry*; VCH: Weinheim, 1990.
(17) (a) McRae, E. G. *J. Phys. Chem.* **1957**, *61*, 562. (b) Paley, M. S.; Harris, J. M.; Looser, H.; Baumert, J. C.; Bjorklund, G. C.; Jundt, D.; Twieg, R. J. *J. Org. Chem.* **1989**, *54*, 3774.
(18) Bakhshiev, N. G; Knyazhanskii, M. I; Minkin, V. I.; Osipov, O. A.; Seidov, G. V. *Russ. Chem. Rev.* **1969**, *3*, 740.
(19) Würthner, F.; Effenberger, F.; Wortmann, R.; Krämer, P. *Chem. Phys.* **1993**, *173*, 305.

field E_0, φ is the angle between the direction of E_0 and the electric field vector of the incident light, and ν is the wavenumber (cm^{-1}) associated with the transition. The measurements are made for two field directions, $\varphi = 0°$ (parallel) and 90° (perpendicular), and several wavenumbers within the charge-transfer band. Figures 7−11 show the electrooptical absorption spectra ($L\epsilon/\nu$) for **2**−**6**, together with their unperturbed analogs (ϵ/ν).

With the exception of **5**, the charge-transfer bands are well separated from other transitions, and in all cases the electrooptical spectra can be fitted numerically,[20] yielding the ground state and excited state dipole moments as well as the direction of the transition dipole moment (μ_{ge}) in the fixed molecular frame. The UV−vis spectrum of the molecule is utilized[21] to determine μ_{ge} from the integrated absorption according to

$$\int \epsilon(\nu)\, d\nu = 2\pi^2 N_A \mu_{ge}{}^2/(6 \ln 10 hc\epsilon_0) \qquad (4)$$

where N_A is Avogadro's number, h Planck's number, and c the speed of light (the integration is carried out over the entire band). The results of EOA experiments are summarized in Table 1, and the details are provided in the Experimental Section.

Compounds **2**−**6** were also studied by electric field induced second harmonic (EFISH) generation at 1907 nm in chloroform solution as described previously.[22] The measured molecular hyperpolarizabilities (β) are presented in Table 1.

The ground state dipole moments of the spiro compounds (as shown by PM3 calculations[12]) point from the dicarbonyl moiety (positive end) to the heteroatoms of the donor moiety (negative end) and are aligned mainly along the long molecular axis. This polarization is reflected in distortions observed in the solid state (see above). The independently determined ground state dipole moments[23] agree very well with those measured by EOA. Also, the calculated values are in reasonable agreement with experimental values. The spiro dyes show moderate polarity in their ground states; the observed μ_g values for all the compounds span a narrow range from 2.3 to 5.5 D (Table 1).

The transition dipole moments (μ_{ge}) are in the direction of the ground state dipole moments, and their magnitudes reflect the symmetries of the donor components. As discussed above, the HOMOs of the phenyl-based donors **1** and **4** have incorrect symmetry for interaction with the LUMO of the dione moiety. The values of μ_{ge} are less than 1 D. For correct-symmetry naphthyl-based donors, the interaction between the frontier orbitals is stronger, yielding μ_{ge} values around 3 D. For comparison, *p*-nitroaniline[24] (PNA), which has directly conjugated donor and acceptor groups of strength similar to that of our spiro components, has a transition dipole of 4.4 D for its CT band, and the bimolecular CT complex[25] of tetracyanoethylene with hexamethylbenzene (TCE−HMB) has $\mu_{ge} = 3.5$ D. Thus, the perpendicular π-systems of correct symmetry can electronically couple with a significant strength. The biphenyl donor **3**, because of geometrical constraints, has diminished overlap between the crucial p orbitals of the carbonyl carbons and the lone pair orbitals on the nitrogens (Figure 6). In addition to the extinction coefficient being lower (see above) the CT band is significantly narrower in this case, leading to a transition dipole that is only 1.7 D. The band widths at half-height (σ in Table 1) follow a trend that might be associated with the vibronic structure of the spiro dyes. The bands are broadest for the naphthyl derivatives (σ is ca. 6.6×10^3 cm^{-1}), slightly narrower for the compounds with phenyl-based donors (σ is ca. 5.9×10^3 cm^{-1}), and narrowest for the biphenyl compound ($\sigma = 4.9 \times 10^3$ cm^{-1}). Perhaps the seven-membered ring in **3** adds extra rigidity to the structure. For comparison, under the same conditions (acetonitrile), the band width of PNA is 5.2×10^3 cm^{-1} and that of TCE−HMB is 5.5×10^3 cm^{-1}.

The excited state dipole moments are in the direction opposite to that of the ground state dipole moments, exactly as expected if the electron density is transferred from the HOMO localized mainly on the donor moiety to the LUMO limited mostly to the acceptor subchromophore. To a first approximation, the excited state should resemble a radical cation/radical anion pair.[8] The magnitudes of the excited state dipoles are, however, relatively small (see below).

Using Mulliken theory,[8,26] we can describe the ground state wave function $|g\rangle$ and the excited state wave function $|e\rangle$ as a linear combination of neutral ($|n\rangle$) and fully ionic ($|i\rangle$) wave functions with a mixing coefficient c:

$$|g\rangle = (|n\rangle + c|i\rangle)/(1 + c^2)^{0.5} \qquad (5)$$

$$|e\rangle = (c|n\rangle - |i\rangle)/(1 + c^2)^{0.5} \qquad (6)$$

These functions are orthonormal if $\langle n|i\rangle = 0$. Since the overlap of molecular orbitals of the subchromophores is rather small, we can assume $\langle n|i\rangle \approx 0$, and accordingly that $\langle n|\mu|i\rangle \approx 0$, where μ is the dipole moment operator. With these approximations one obtains expectation values for the ground state ($\langle g|\mu|g\rangle = \mu_g$) and excited state ($\langle e|\mu|e\rangle = \mu_e$) dipole moments, as well as expressions for the transition dipole ($\langle e|\mu|g\rangle = \mu_{ge}$) and the change of dipole moment upon excitation ($\Delta\mu$):

$$\langle g|\mu|g\rangle = (\langle n|\mu|n\rangle + c^2\langle i|\mu|i\rangle)/(1 + c^2) \qquad (7)$$

$$\langle e|\mu|e\rangle = (c^2\langle n|\mu|n\rangle + \langle i|\mu|i\rangle)/(1 + c^2) \qquad (8)$$

$$\langle e|\mu|g\rangle = -c\Delta/(1 + c^2) \qquad (9)$$

$$\Delta\mu = (1 - c^2)\Delta/(1 + c^2) \qquad (10)$$

where Δ is the maximum possible change of the dipole moment ($\Delta = \langle i|\mu|i\rangle - \langle n|\mu|n\rangle$).

Using the data of Table 1, the mixing coefficients and Δ values can be estimated for all spiro dyes. The mixing coefficient can be used as a measure of spiroconjugation between the donor and acceptor moieties. For compounds with donors of correct symmetry (**2**, **3**, **5**, and **6**), the ionic structure contributes just above 6% ($c^2/(1 + c^2)$) to the description of the molecule, while in the phenyl-based compounds of incorrect symmetry that contribution is close to 1% (Table 1). For comparison, PNA[24] (where the approximation that $\langle n|i\rangle = 0$ is probably not valid) has $c = 0.73$ (35%), and in the TCE−HMB

(20) (a) Liptay, W. In *Excited States*; Lim, C., Ed.; Academic Press: New York, 1974; Vol. I, p 129. (b) Wortmann, R.; Elich, K.; Lebus, S.; Liptay, W.; Borowicz, P, Grabowska, A. *J. Phys. Chem.* **1992**, *96*, 9724.

(21) Liptay, W. *Angew. Chem., Int. Ed. Engl.* **1969**, *8*, 177.

(22) (a) Levine, B. F.; Bethea, C. G. *J. Chem. Phys.* **1975**, *63*, 2666. (b) Oudar, J. L. *Chem. Phys.* **1977**, *67*, 466. (c) Moylan, C. R.; Miller, R. D.; Twieg, R. J.; Betterton, V. Y.; Matray, T. J.; Ngyuyen, C. *Chem. Mater.* **1993**, *5*, 1499.

(23) The ground state dipole moments were determined from dielectric and refractive index measurements according to the Guggenheim expression: Guggenheim, E. A. *Trans. Faraday Soc.* **1949**, *45*, 714.

(24) Wortmann, R.; Krämer, P.; Glania, C.; Lebus, S.; Detzer, N. *Chem. Phys.* **1993**, *173*, 305.

(25) Liptay, W.; Rehm, T.; Wehning, D.; Schanne, L.; Baumann, W.; Lang, W. *Z. Naturforsch.* **1982**, *37a*, 1427.

(26) For a similar approach to intermolecular CT complexes see: Di Bella, S.; Fragalá, I. L.; Ratner, M. A.; Marks, T. J. *J. Am. Chem. Soc.* **1993**, *115*, 682.

complex (μ_g = 1.9 D, μ_e = 6.6 D, μ_{ge} = 3.5 D)[25] the contribution of the ionic structure is 18% (c = 0.47, Δ = 8.5 D).

Incidentally, the data for the TCE−HMB complex also allow for a straightforward test of the CT model. The result for the matrix element $\langle n|\mu|n\rangle$ which can be calculated from eqs 7−10 is zero within experimental error. This is exactly the prediction of the CT model since $\langle n|\mu|n\rangle$ represents the total dipole moment of the two noninteracting subchromophores and both TCE and HMB are nonpolar. The ground state dipole of the sandwich complex is, therefore, entirely due to admixtures of the ionic wave function $|i\rangle$ to the neutral wave function $|n\rangle$.

Within that simple CT model the excited states of the spiro compounds are indeed well described as the radical anion/radical cation pair. The degree of electron transfer accompanying the transitions ($(1 - c^2)/(1 + c^2)$) is more than 90% in all the compounds. The moderate magnitudes of the excited state dipole moments (μ_e from −2 to −8 D) can thus be traced to the small distances between the separated charges, rather than to a small degree of the charge transfer. This conclusion has important implications for the design of the next generation of spiro dyes (see below).

Using the two-state model[27] and the data obtained from EOA measurements we can estimate the CT contribution to the molecular hyperpolarizability, β(CT), for the spiro dyes:

$$\beta(\mathrm{CT}) = \frac{3\mu_{ge}^{\,2}\Delta\mu}{h^2c^2\omega_{max}^{\,2}} \frac{\omega_{max}^{\,4}}{(\omega_{max}^{\,2} - \omega^2)(\omega_{max}^{\,2} - 4\omega^2)} \quad (11)$$

where ω is the laser frequency and ω_{max} the frequency corresponding to the maximum of the CT transition. The absolute magnitudes of calculated values are the largest for the naphthyl derivatives **2** and **5** (Table 1), and the smallest for the phenyl analogs **1** and **4**. In general the calculated values do not agree with the measured data. The EFISH data represent the total molecular hyperpolarizability;[22,28] i.e., all transitions contribute to the molecular response. The calculated values are based explicitly and exclusively on CT band contributions. The differences between the observed values and the calculated CT contributions ($\Delta\beta$) are relatively constant for **2**−**5** (12.6×10^{-30} esu on the average), indicating that there is a dominant second transition that contributes to the molecular hyperpolarizability. This transition is common to these dyes, and it provides a contribution that is in the direction opposite to that from the CT transition. It is very likely that the acceptor subchromophore is responsible for this "destructive" interference. EFISH measurements on 1,3-indandione gave β(1.907 μm) = 11.6(7) $\times 10^{-30}$ esu in support of this conclusion. Additional support is provided by **6**, where the methoxy substituents act as the second internal donor, and the acceptor's contribution becomes quite strong ($\Delta\beta = 39.5 \times 10^{-30}$ esu).

The compounds presented here provide examples of a new class of organic dyes that are based on intramolecular interactions between nearly orthogonal subchromophores. The spiro-conjugation used to couple the two π-subsystems electronically provides a reasonably strong mode of interaction and leads to CT transitions with modest probabilities. The inversion of the dipole moments upon transition leads to significant changes of the dipole moments, providing a starting point for the design of compounds with large molecular hyperpolarizibilities. The next generation of spiro dyes should have subchromophores that would bring the frontier orbitals of the subchromophores closer in energy, increase their overlap, separate charges over larger distances, and properly align the transitions within subchromophores to avoid the cancellation of various contributions. Preparation of such dyes is in progress.

Experimental Section

Unless otherwise noted, all materials were obtained from Aldrich Chemical Co., Inc., and used without purification. Reagent grade diethyl ether and tetrahydrofuran were distilled from potassium/benzophenone under argon immediately before use under anhydrous conditions. Reagent grade methylene chloride and spectrophotometric grade benzene were distilled from calcium hydride under argon immediately before use under anhydrous conditions. Aldrich anhydrous grade (Sure-Seal) acetonitrile, dimethyl sulfoxide, dimethylformamide and dimethylacetamide were used for preparative work when needed in anhydrous form. The solvents used for UV/vis and fluorescence spectroscopies were spectrophotometric grade and used without further purification. Pyridine was dried overnight over solid sodium hydroxide and then distilled under argon from the hydroxide onto 4 Å molecular sieves for storage.

All ^{1}H and ^{13}C spectra were obtained using one of the following Bruker spectrometers: a AC-200 or WP-200 (200 MHz for proton), an AM-300 (300 MHz for proton), or a WP-360 (360 MHz for proton). ^{1}H and ^{13}C chemical shifts are reported in parts per million with respect to tetramethylsilane (0.00 ppm). $CDCl_3$ was used as the solvent for ^{1}H and ^{13}C NMR, unless otherwise noted. All of the ^{13}C spectra were recorded with high-power, broad-band decoupling.

Mass spectra were recorded using one of the following Kratos instruments: a MS-950 double-focusing mass spectrometer in the electron-impact mode (reported as EI-MS) or a MS-25 double-focusing mass spectrometer for chemical ionization using isobutylene as the ionization gas (reported as CI-MS). Mass spectral data are expressed as *m*/*z* (intensity as the percent of the most abundant ion peak). All observed peaks with masses above *m*/*z* 80 and more intense than 10% of the most abundant ion peak as well as peaks judged to be of particular significance are reported.

All UV/vis absorbance spectra were obtained using a Hewlett-Packard 8452A diode array spectrometer at ambient temperatures. Fluorescence measurements were made using a Spex Fluorometer. Infrared spectra were obtained using a Perkin-Elmer 1600 series FTIR spectrometer (reported as FTIR).

The solvatochromic data for the spiro compounds were obtained in benzene, dioxane, toluene, CH_2Cl_2, THF, pyridine, acetone, acetonitrile, and dimethyl sulfoxide. The physical data for the solvents were obtained from the *Handbook of Organic Photochemistry*.[29] The observed wavelengths for the maxima of charge transfer bands are listed below (according to the solvent list above), followed by *a* values (Å, taken as 0.71*L*/2, where *L* is the largest atom-to-atom distance in the molecule) and *B* values ($\times 10^{-13}$ s^{-1}) obtained from the regression analysis. **1**: 580, 560, 582, 552, 558, −, 540, 536, 546; 4.0; 5.1(5). **2**: 428, 420, 424, 414, 414, 412, 404, 400, 410; 4.2; 4.1(5). **3**: 428, −, 428, 420, −, −, 418, 414, 418; 4.2; 2.6(4). **4**: 480, −, −, 472, 472, −, 468, 466, 470; 4.1; 2.0(1). **6**: 392, −, −, 382, 374, −, 368, 370, −; 4.9; −1.8(6).

Preparative flash column chromatography[30] was performed using Merck silica gel 60 (230−400 mesh). TLC was done on Merck precoated plates (60F-254) with a layer thickness of 0.25 mm. All solvents used for thin-layer and flash column chromatographies were reagent grade.

Crystal, data collection, and refinement parameters are given in Table 2. Suitable crystals were selected and mounted on glass fibers with epoxy cement. The unit-cell parameters were obtained by the least-squares refinement of the angular settings of 24 reflections ($20° \le 2\theta \le 24°$).

The systematic absences in the diffraction data are uniquely consistent for the reported space groups. The structures were solved using direct methods, completed by subsequent difference Fourier

(27) (a) Oudar, J. L.; Chemla, D. S. *J. Chem. Phys.* **1977**, *66*, 2664. (b) Oudar, J. L. *J. Chem. Phys.* **1977**, *67*, 446.

(28) (a) Zyss, J.; Oudar, J. L. *Phys. Rev. A* **1982**, *26*, 2016. (b) Moylan, C. R. *J. Chem. Phys.* **1993**, *99*, 1436.

(29) Scaiano, J. C., Ed. *Handbook of Organic Photochemistry*; CRC Press: Boca Raton, FL, 1989; Vol. II, p 344.

(30) Still, W. G.; Kahn, M.; Mitra, A. *J. Org. Chem.* **1978**, *43*, 2923.

Table 2. Crystallographic Data for **2**, **4**, **5**, and **6**

	2	**4**	**5**	**6**
		(a) Crystal Parameters		
formula	$C_{21}H_{16}N_2O_2$	$C_{16}H_{11}NO_2S$	$C_{20}H_{13}NO_2S$	$C_{23}H_{20}N_2O_4$
formula weight	328.4	281.3	331.4	388.4
crystal system	orthorhombic	orthorhombic	orthorhombic	monoclinic
space group	*Pbca*	*Pbca*	*Pbca*	$P2_1/n$
a (Å)	22.413(8)	22.086(7)	23.017(16)	9.519(2)
b (Å)	16.696(6)	15.888(7)	16.109(3)	12.642(2)
c (Å)	8.512(2)	7.553(3)	8.273(2)	15.950(5)
β (deg)				100.95(2)
V (Å^3)	3185(2)	2651(2)	3068(1)	1884.4(7)
Z	8	8	8	4
cryst dimens (mm)	0.1 × 0.4 × 0.4	0.4 × 0.4 × 0.4	0.2 × 0.2 × 0.4	0.2 × 0.2 × 0.3
cryst color	red	red-orange	orange	orange
D(calc) (g cm^3)	1.369	1.410	1.435	1.370
μ(Mo Kα) (cm^{-1})	0.89	2.44	2.23	0.94
temp (K)	295	293	242	250
		(b) Data Collection		
diffractometer		Siemens P4		
monochromator		graphite		
radiation		Mo Kα (λ = 0.710 73 Å)		
2θ scan range (deg)	4.0−48.0	4.0−50.0	4.0−48.0	4.0−42.0
data collected (h,k,l)	+25, +19, +9	+26, +18, +8	+26, +18, +9	±9, +12, +16
rflns collected	2521	2444	2554	2110
indpt rflns	2313	2323	2426	2023
indpt obsvd rflns [$F_o \geq 4\sigma(F_o)$]	1236	1539	1552	1449
		(c) Refinement[a]		
$R(F)$ (%)	5.41	4.91	4.25	7.23
$R(wF)$ (%)	6.32	6.41	6.98	9.58
Δ/σ (max)	0.04	0.03	0.00	0.00
$\Delta(\rho)$ (eÅ^{-3})	0.3	0.4	0.2	0.5
N_o/N_v	5.5	8.5	7.2	9.9
GOF	1.2	1.2	1.6	1.5

[a] Quantity minimized = $\sum w\Delta^2$; $R = \sum\Delta/\sum(F_o)$; $R(w) = \sum\Delta w^{1/2}/\sum(F_o w^{1/2})$, $\Delta = |(F_o - F_c)|$.

syntheses and refined by full-matrix least-squares procedures. Absorbtion corrections were ignored because of <10% variation of the integrated ψ-scan intensities. Carbon atoms in **6** were refined isotropically. All remaining non-hydrogen atoms were refined with anisotropic displacement coefficients. Hydrogen atoms were treated as idealized contributions. All software and sources of scattering factors are contained in the SHELXTL Plus (4.2) program library (G. Sheldrick, Siemens XRD, Madison, WI).

The electrooptical absorption measurements (EOAM) were performed as described previously.[19,20] All measurements were made in dioxane which was carefully purified and dried by distillation from sodium/potassium alloy prior to use. Accurate UV/vis spectra which are required for the numerical analysis of the EOAM data were recorded on a Perkin-Elmer 340 spectrophotometer.

The EFISH measurements were performed as previously described.[22] Solutions at three different concentrations of each compound were prepared, and second harmonic generation was detected with an applied electric field of 2×10^4 V/cm. The fundamental wavelength was 1907 nm, obtained by Raman shifting of the 1064 nm YAG fundamental in hydrogen. The EFISH results were referenced to a quartz standard, whose second harmonic coefficient d_{11} at 1907 nm is 6.7×10^{-10} esu. The B convention for β of Willets et al. was used.[39]

As part of the determination of the product $\mu\beta$ for each chromophore, the concentration dependence of the dielectric constant was determined. That concentration dependence was also used to determine the dipole moment independently. From the $\mu\beta$ product derived from the EFISH measurements, and the value of μ obtained from the dielectric measurements, β at 1907 nm was determined. UV/vis spectra were recorded on a diode array spectrophotometer (±2 nm) in dilute chloroform solution.

5,6-Dimethoxy-2,2,3,3-tetrabromoindan-1-one was prepared by benzylic bromination followed by enolic bromination of 5,6-dimethoxyindan-1-one (R_f = 0.17, 30% ethyl acetate in hexane). *N*-Bromosuccinimide (4.0 g, 22 mmol) and 20 mg of azobisisobutyronitrile were added to a solution of 5,6-dimethoxyindan-1-one (2.0 g, 10 mmol) in 100 mL of carbon tetrachloride under an argon atmosphere. The mixture was heated at reflux, and the reaction was followed by TLC and NMR. After 90 min of refluxing, there was no starting material left and NMR showed 5,6-dimethoxy-3,3-dibromoindan-1-one as the only product (R_f = 0.52, 30% ethyl acetate in hexane). ^{1}H NMR ($CDCl_3$, 200 MHz): δ 7.32 (s, 1 H), 7.09 (s, 1 H), 4.11 (s, 3 H), 3.98 (s, 3 H), 3.94 (s, 2 H). The reaction mixture was cooled to room temperature, and then a solution of bromine (3.5 g, 0.022 mol) in 20 mL of carbon tetrachloride was added dropwise over a 30 min period with vigorous stirring. After the addition was complete, the mixture was brought to reflux and the reaction was followed by NMR. After 2−3 h of refluxing, NMR showed the desired tetrabromide as the only product. The mixture was cooled to room temperature and filtered, and the filtered solids were washed with carbon tetrachloride. The combined organic layers were then washed with water (3 × 100 mL) and saturated sodium chloride solution (100 mL), dried over sodium sulfate, and filtered. The filtrate was removed under reduced pressure to yield the tetrabromide (5.07 g, 96%) as a yellow solid (R_f = 0.52, 30% ethyl acetate in hexane) which was used for the next reaction without further purification. ^{1}H NMR ($CDCl_3$, 200 MHz): δ 7.25 (s, 1 H), 7.18 (s, 1 H), 4.09 (s, 3 H), 3.97 (s, 3 H).

5,6-Dimethoxy-2,2-dibromoindan-1,3-dione was prepared by the silver nitrate hydrolysis of 5,6-dimethoxy-2,2,3,3-tetrabromoindan-1-one. A solution of $AgNO_3$ (4.25 g, 0.025 mol) in 4 mL of water was added to a solution of the bromide (5.08 g, 0.01 mol) in 50 mL of acetonitrile, and the mixture was heated at reflux. A yellow-white precipitate fell out of solution immediately, and refluxing was continued for 1 h. After cooling to room temperature, the mixture was filtered and the filtered solids were washed well with acetonitrile. The combined filtrates were removed by rotary evaporation, and the white solid thus obtained was suspended in 100 mL of methylene chloride. This solution was filtered to remove any remaining silver salts, and the filtrate was evaporated to yield the dione (3.41 g, 94%) as a white solid (R_f = 0.37, 30% ethyl acetate in hexane) which was used in the next reaction without further purification. ^{1}H NMR ($CDCl_3$, 300 MHz): δ 7.41 (s, 2 H), 4.10 (s, 6 H). ^{13}C NMR ($CDCl_3$, 75 MHz): δ 186.4, 157.8, 130.6, 105.0, 57.0, 51.8. EI-MS: m/z 366 (M^+ + 4,

49), 364 ($M^+ + 2$, 100), 362 (M^+, 51), 285 ($M^+ + 2 - Br$, 32), 283 ($M^+ - Br$, 30), 255 ($M^+ - Br - CO$, 23).

5,6-Dimethoxyninhydrin[31] was prepared by the dimethyl sulfoxide hydrolysis of 5,6-dimethoxy-2,2-dibromoindan-1,3-dione. A solution of the dione (2.0 g, 5.5 mmol) in 20 mL of anhydrous dimethyl sulfoxide was heated at 90−95 °C for a period of 2 days under an argon atmosphere. The reaction was followed by TLC and stopped upon disappearance of starting material. After cooling to room temperature, the mixture was poured into 200 mL of water and then extracted with ethyl acetate (5 × 100 mL). The combined organic layers were dried over sodium sulfate, filtered, and evaporated under reduced pressure to yield a yellow oil. The oil was purified by column chromatography using a mixture of 4% methanol in methylene chloride as the eluant to yield the ninhydrin (0.78 g, 59%) as a light yellow oil ($R_f = 0.41$, 5% methanol in methylene chloride). ^{1}H NMR (acetone-d_6, 300 MHz): δ 7.37 (s, 2 H), 6.30 (s, 2 H, D_2O exchangeable), 4.06 (s, 6 H). EI-MS: *m*/*z* 238 (M^+, 2), 220 ($M^+ - H_2O$, 16), 192 ($M^+ - H_2O - CO$, 30), 164 ($M^+ - H_2O - 2CO$, 100), 136 ($M^+ - H_2O - 3CO$, 79).

***N,N′*-Dimethyl-1,2-phenylenediamine** was prepared by the method of Cheeseman.[32]

***N,N′*-Bis(*p*-tolylsulfonyl)-2,2′-diaminobiphenyl** was obtained by tosylation of 2,2′-diaminobiphenyl.[33] A solution of *p*-toluenesulfonyl chloride (19 g, 0.1 mol) in 50 mL of anhydrous pyridine was added slowly to a solution of 2,2′-diaminobiphenyl (9.2 g, 0.05 mol) in 25 mL of anhydrous pyridine under an argon atmosphere so that the temperature of the reaction mixture did not exceed 60 °C. After stirring overnight, the reaction mixture was poured slowly into 500 mL of 15% hydrochloric acid with vigorous stirring to give a gray solid. After stirring for 1 h the solid was filtered, washed well with water, and dried under vacuum. Upon recrystallization from acetic acid, white crystals of the desired tosyl amide (21.9 g, 89%) were obtained. ^{1}H NMR ($CDCl_3$, 200 MHz): δ 7.66 (dd, $J = 8$, 1 Hz, 2 H), 7.50 (d, $J =$ 8 Hz, 4 H), 7.33 (m, 2 H), 7.24 (d, $J = 8$ Hz, 4 H), 7.05 (m, 2 H), 6.48 (dd, $J = 8$, 1 Hz, 2 H), 5.90 (s, 2 H), 2.42 (s, 6 H).

***N,N′*-Dimethyl-*N,N′*-bis(*p*-tolylsulfonyl)-2,2′-diaminobiphenyl.** The above diamide (12.25 g, 0.025 mol) was refluxed with 4 N aqueous NaOH (12.5 mL, 0.05 mol) for 5 min. The mixture was cooled in an ice bath (0−5 °C), and then dimethyl sulfate (4.5 mL, 0.05 mol) was added dropwise. After the initial reaction had subsided, the mixture was gently boiled for 5 min. After cooling, the suspended solid was crushed and 12.5 mL of 4 N aqueous NaOH and 4.5 mL of dimethyl sulfate were added. The mixture was boiled again for 5 min. After two further similar treatments, the solid was filtered from the hot mixture and then boiled with 200 mL of 0.75 N aqueous NaOH solution. The insoluble material was filtered and recrystallized from 95% ethanol to yield *N,N′*-dimethyl-*N,N′*-bis(*p*-tolylsulfonyl)-2,2′-diaminobiphenyl (10.87 g, 84%) as colorless needles ($R_f = 0.41$, methylene chloride). ^{1}H NMR ($CDCl_3$, 200 MHz): δ 7.32 (m, 14 H), 6.78 (dd, $J = 8$, 1 Hz, 2 H), 3.05 (s, 6 H), 2.43 (s, 6 H).

***N,N′*-Dimethyl-2,2′-diaminobiphenyl** was prepared by the hydrolysis of the corresponding tosyl amide. The dimethyl diamide (5.6 g, 0.011 mol) was heated at 120 °C in a mixture of glacial acetic acid (3 mL) and concentrated sulfuric acid (3 mL) under an argon atmosphere for 2 h. The reaction was followed by TLC (aliquots were worked up as mentioned later and extracted with ether, and the ether extract was used as the sample for TLC) and stopped upon disappearance of starting material. After cooling to room temperature, the reaction mixture was poured into 50 mL of ice−water. Slow addition of 10 N aqueous NaOH solution was carried out till the solution was slightly basic, and the mixture was immediately diluted to a final volume of 300 mL. The mixture was extracted with ether (4 × 100 mL). The combined organic layers were dried over sodium sulfate and then evaporated under reduced pressure to yield the desired amine (1.83 g, 81%) as a light yellow solid ($R_f = 0.74$, methylene chloride; $R_f = 0.85$, 40% ethyl acetate in hexane). ^{1}H NMR (acetone-d_6, 360 MHz): δ 7.21 (m, 2 H), 6.93 (m, 2 H), 6.68 (m, 2 H), 4.0 (s, 2 H, D_2O exchangeable), 2.76 (s, 6 H). EI-MS: *m*/*z* 212 (M^+, 47), 211 ($M^+ - H$, 32), 210 ($M^+ -$ 2H, 24), 197 ($M^+ - CH_3$, 13), 196 ($M^+ - CH_3 - H$, 34), 195 ($M^+ - CH_3 - 2H$, 26), 182 ($M^+ - 2CH_3$, 40), 181 ($M^+ - 2CH_3 - H$, 96), 180 ($M^+ - 2CH_3 - 2H$, 100), 167 ($M^+ - 2CH_3 - NH$, 41), 166 ($M^+ - 2CH_3 - NH - H$, 14), 152 ($M^+ - 2CH_3 - 2NH$, 16).

1,2-Dimethylperimidine was prepared by a modified procedure of Pozharskii.[34] Iodomethane (46.88 g, 0.33 mol) was added dropwise over a period of 10 min to a solution of 2-methylperimidine[35] (30.0 g, 0.165 mol) in 60 mL of dimethylformamide at 100 °C (Baker spectrophotometric grade), containing finely powdered potassium carbonate (22.75 g, 0.165 mol). The mixture was heated for 30 min, giving a yellow precipitate. After cooling, the yellow solid was filtered and suspended in 1500 mL of water. Aqueous ammonium hydroxide was added slowly with vigorous stirring till the solution was slightly basic to litmus. During the course of addition, a yellow-green solid appeared. The solid was filtered, washed with water, and dried under vacuum to give the desired product (20.8 g, 65%). The dimethylformamide filtrate from the first filtration was added to 1200 mL of water, and the solution was made alkaline with aqueous ammonium hydroxide to yield a yellow-green solid. The solid was filtered, washed with water, and dried under vacuum to give an additional 7.8 g (24%) of product. The product was used in the next reaction without purification. ^{1}H NMR ($CDCl_3$, 200 MHz): δ 7.20 (m, 4 H), 6.85 (dd, $J = 7$, 1 Hz, 1 H), 6.24 (dd, $J = 6$, 2 Hz, 1 H), 3.21 (s, 3 H), 2.35 (s, 3 H).

1,2-Dimethylperimidinyl methiodide was prepared in a manner similar to that of Pozharskii.[34] Iodomethane (30.2 g, 0.21 mol) was added in one portion to a solution of 1,2-dimethylperimidine (20.8 g, 0.106 mol) in dimethylformamide (80 mL) at 100 °C. The mixture was heated for 20 min, giving a yellow solid. After cooling, the solid was filtered and dried under vacuum to give the desired salt (29.5 g, 82%) which was used in the next reaction without purification. ^{1}H NMR (dimethyl sulfoxide-d_6, 200 MHz): δ 7.66 (dd, $J = 8$, 1 Hz, 2 H), 7.54 (t, $J = 8$ Hz, 2 H), 7.24 (dd, $J = 8$, 1 Hz, 2 H), 3.61 (s, 6 H), 2.78 (s, 3 H).

1,8-Bis(methylamino)naphthalene was prepared according to the method of Pozharskii.[36] Argon was bubbled through a solution of potassium hydroxide (76.5 g) in 95% ethanol (425 mL) for 5 min. The methiodide salt (17 g, 0.05 mol) was added in one portion to the alkaline ethanol and refluxed under an argon atmosphere. After 2 h, the reaction mixture was cooled and diluted with water to yield a final volume of 2 L. The obtained solution was neutralized with glacial acetic acid till it was weakly basic to litmus. A brown solid precipitated out during this time. This solid was filtered, washed with water, and dried under vacuum to yield the desired amine (7.23 g, 78%). Light yellow prisms of the product were obtained upon recrystallization from 95% ethanol; mp 100 °C (lit.[37] mp 101 °C); $R_f = 0.42$, 10% ethyl acetate in hexane. ^{1}H NMR ($CDCl_3$, 200 MHz): δ 7.27 (dd, $J = 8$, 7 Hz, 2 H), 7.18 (dd, $J = 8$, 1 Hz, 2 H), 6.57 (dd, $J = 7$, 1 Hz, 2 H), 5.45 (s, 2 H, D_2O exchangeable), 2.87 (s, 3 H). EI-MS: *m*/*z* 186 (M^+, 100), 185 ($M^+ -$ H, 6), 171 ($M^+ - CH_3$, 15), 170 ($M^+ - CH_3 - H$, 18), 169 ($M^+ - CH_3 - 2H$, 41), 156 ($M^+ - 2CH_3$, 14), 155 ($M^+ - 2CH_3 - H$, 15), 154 ($M^+ - 2CH_3 - 2H$, 53), 141 ($M^+ - 2CH_3 - NH$, 4), 140 ($M^+ - 2CH_3 - NH - H$, 8), 126 ($M^+ - 2CH_3 - 2NH$, 9).

2-(Methylamino)benzenethiol was prepared using an approach similar to that of Kiprianov.[37] Argon was bubbled through a solution of *N*-methylbenzothiazole-2-thione (Janssen Chimica; 0.534 g, 3 mmol) in hot (60 °C) 95% ethanol (1.55 mL) for 5 min. A solution of potassium hydroxide (0.504 g, 9 mmol) in 95% ethanol (1.55 mL) was added in one portion and the mixture was heated at reflux under an argon atmosphere. After 2 h, the reaction mixture was cooled to room temperature even though TLC showed the presence of starting material. The mixture was diluted with water to yield a final volume of 30 mL. The obtained solution was neutralized with concentrated hydrochloric acid till it was weakly basic to litmus and then extracted with benzene

(31) (a) Lennard, C. J.; Margot, P. A.; Stoilovic, M.; Warrener, R. N. *J. Forensic Sci*. **1986**, *26*, 323. (b) Lennard, C. J.; Margot, P. A.; Stoilovic, M.; Warrener, R. N. *Forensic Sci. Soc.* **1988**, *28*, 3. (c) Kametani, T.; Hibino, S.; Takano, S. *J. Chem. Soc., Perkin Trans. 1* **1972**, 391. (d) Almog, J.; Hirshfeld, A. *J. Forensic Sci*. **1988**, *33*, 1027.

(32) Cheeseman, G. W. H. *J. Chem. Soc.* **1955**, 3308.

(33) Moore, R. E.; Furst, A. *J. Org. Chem.* **1958**, *23*, 1504.

(34) Sokolov, V. I.; Ardashev, B. I.; Kashparov, I. S.; Pozharskii, A. F. *Khim. Geterosikl. Soedin.* **1973**, 849

(35) Whitehurst, J. S. *J. Chem. Soc*. **1951**, 226.

(36) Pozharskii, A. F.; Suslov, A. N.; Starshikov, N. M.; Popova, L. L.; Klyuev, N. A.; Adanin,V. A. *Zh. Org. Khim.* **1980**, *16*, 2216.

(37) Kiprianov, A. I.; Pazenko, Z. N. *Zh. Obshch. Khim.* **1949**, *19*, 1523.

(3 × 25 mL). The benzene extracts were used for the next reaction without further purification. An aliquot of the benzene layer was concentrated by rotary evaporation and dried under vacuum to yield a light yellow oil. NMR of this oil showed a 1:1 mixture of the desired amino thiol (R_f = 0.84, 20% ethyl acetate in hexane) and the starting material (R_f = 0.63, 20% ethyl acetate in hexane).

***N*-Methyl-1,8-naphthosultam** was prepared by the alkylation of 1,8-naphthosultam (R_f = 0.38, 30% ethyl acetate in hexane; R_f = 0.11, 60% methylene chloride in hexane) with iodomethane. A solution of sodium hydroxide (0.42 g, 10.5 mmol) in 10 mL of water was added, with stirring, to a solution of 1,8-naphthosultam (2.05 g, 10 mmol) in 10 mL of dimethylacetamide under an argon atmosphere. The mixture became warm upon addition of base and was allowed to cool to room temperature. Iodomethane (0.65 mL, 10.5 mmol) was then added to the mixture, and the resulting solution was stirred for 2 h. Reaction progress was followed by TLC, and the reaction was stopped upon complete disappearance of the starting material. The reaction mixture was poured slowly into 150 mL of water, with vigorous stirring, yielding a gray-white solid. After stirring for 30 min, the solid was filtered, washed with water, and dried under vacuum. Upon recrystallization from 20% ethyl acetate in hexane, white crystals of *N*-methyl-1,8-naphthosultam (1.56 g, 71%) were obtained (R_f = 0.55, 30% ethyl acetate in hexane; R_f = 0.36, 60% methylene chloride in hexane). ^{1}H NMR ($CDCl_3$, 300 MHz): δ 8.07 (dd, J = 8, 1 Hz, 1 H), 7.97 (dd, J = 7, 1 Hz, 1 H), 7.75 (dd, J = 8, 7 Hz, 1 H), 7.55 (t, J = 8 Hz, 1 H), 7.46 (dd, J = 8, 1 Hz, 1 H), 6.72 (dd, J = 7, 1 Hz, 1 H), 3.38 (s, 3 H). EI-MS: m/z 219 (M^+, 10), 155 ($M^+ - SO_2$, 5), 126 (M^+ − NMe − SO_2, 3), 64 (SO_2^+, 17).

8-(Methylamino)-1-naphthalenethiol was prepared by the $LiAlH_4$ reduction of the sultam from the previous step. A solid addition funnel was used to deliver the sultam (0.15 g, 0.68 mmol) slowly, over a 10 min period, to a stirred solution of $LiAlH_4$ (0.026 g, 6.8 mmol) in 20 mL of dry ether under an argon atmosphere. The resulting solution was refluxed overnight and then cooled to room temperature. Ethyl acetate (*ca.* 10 mL) was added dropwise, with vigorous stirring, to the reaction mixture till no more gas was evolved. A solution of 3 M sulfuric acid (10 mL) was added slowly to the reaction mixture, and after stirring for 15 min, the ether layer was removed. The aqueous layer was extracted with benzene (3 × 20 mL) while it was still under the argon atmosphere. The combined organic extracts were used immediately for the next reaction due to the ease with which the product is oxidized upon exposure to air. An aliquot of the benzene layer was evaporated under reduced pressure to give the product (R_f = 0.36, 30% ethyl acetate in hexane) as a light yellow oil. ^{1}H NMR ($CDCl_3$, 200 MHz): δ 7.63 (dd, J = 8, 1 Hz, 1 H), 7.34 (m, 2 H), 7.18 (m, 2 H), 6.63 (dd, J = 8, 1 Hz, 1 H), 5.74 (s, 1 H, D_2O exchangeable), 3.41 (s, 1 H, D_2O exchangeable), 2.91 (s, 3 H). EI-MS: m/z 189 (M^+, 15), 188 (M^+ − H, 10), 187 (M^+ − 2H, 54), 174 ($M^+ - CH_3$, 15), 173 (M^+ − H − CH_3, 17), 172 (M^+ − 2H − CH_3, 100).

General Procedure for Preparation of Spiro Compounds. A donor compound was condensed with an equimolar amount of an acceptor compound using benzene (spectrophotometric grade, dried over 4 Å sieves for at least 1 day before use) as solvent and *p*-toluenesulfonic acid as catalyst. The reaction vessel was equipped with a Dean−Stark trap for azeotropic removal of water as it is formed during the reaction. Typically, the donor compound was added to a solution of the acceptor compound and catalyst (*ca.* 5−10 mg) under an argon atmosphere. The scale of this reaction varied from as little as 10 mg to as much as 1 g each of donor and acceptor compounds. The solution was brought to reflux and the reaction followed by TLC using an appropriate amount of ethyl acetate in hexane as the eluant. The reaction was usually complete (marked by disappearance of starting materials on TLC) after 2−5 h of refluxing. The solvent was removed under reduced pressure, and the products[38] were isolated as highly colored solids using flash column chromatography on silica gel with an appropriate amount of ethyl acetate in hexane as the eluant.

Synthesis of 1. The reaction was carried out using 1.00 g of *N*,*N*′-dimethyl-1,2-phenylenediamine and an equimolar amount of ninhydrin. The pure compound was isolated after column chromatography (R_f = 0.42, 40% ethyl acetate in hexane) in 60% yield. Upon recrystallization from benzene, deep purple needles were obtained, mp 142 °C. ^{1}H NMR ($CDCl_3$, 200 MHz): δ 8.10−7.98 (m, 4 H), 6.68−6.65 (m, 2 H), 6.33−6.30 (m, 2 H), 2.61 (s, 6 H). ^{13}C NMR ($CDCl_3$, 50 MHz): δ 198.2, 140.6, 140.5. 137.4, 123.5, 119.3, 104.4, 87.6, 30.7. EI-MS: m/z 278 (M^+, 27), 249 ($M^+ - NCH_3$, 23), 221 ($M^+ - NCH_3 - CO$, 100). FTIR (KBr): 3070 (w), 2878 (w), 2813 (w), 1747 (m), 1717 (s), 1598 (m), 1503 (s), 1403 (w), 1324 (m), 1268 (w), 1238 (m), 1218 (m), 1115 (m), 1015 (m), 932 (s), 878 (w), 774 (m), 741 (s), 711 (m), 676 (w), 607 (w), 561 (w) cm^{-1}.

Synthesis of 2. The reaction was carried out using 1.00 g of 1,8-bis(methylamino)naphthalene and an equimolar amount of ninhydrin. The pure compound was isolated in 64% yield after column chromatography (R_f = 0.51, 40% ethyl acetate in hexane). Recrystallization from 95% ethanol gave red-brown needles, mp 293 °C. ^{1}H NMR ($CDCl_3$, 360 MHz): δ 8.06−7.97 (m, 4 H), 7.35 (dd, J = 8, 7 Hz, 2 H), 7.31 (dd, J = 8, 1 Hz, 2 H), 6.64 (dd, J = 7, 1 Hz, 2 H), 2.80 (s, 6 H). ^{13}C NMR ($CDCl_3$, 50 MHz): δ 199.4, 140.9, 140.3, 137.2, 133.3, 126.7, 123.3, 119.2, 113.2, 105.1, 76.9, 34.5. EI-MS: m/z 328 (M^+, 36), 299 ($M^+ - NCH_3$, 5), 271 ($M^+ - NCH_3 - CO$, 100). CI-MS: m/z 329 ($M^+ + 1$, 84), 328 (M^+, 100), 300 ($M^+ - CO$, 5), 271 ($M^+ - NCH_3 - CO$, 29). FTIR (KBr): 2880 (w), 2810 (w), 1745 (m), 1702 (s), 1582 (s), 1478 (m), 1422 (m), 1390 (w), 1335 (w), 1264 (m), 1220 (w), 1172 (w), 986 (w), 804 (m), 752 (m), 715 (w), 640 (w) cm^{-1}.

Synthesis of 3. The reaction was carried out using 1.00 g of *N*,*N*′-dimethyl-2,2′-diaminobiphenyl and an equimolar amount of ninhydrin. After column chromatography, the product was isolated in a 76% yield (R_f = 0.50, 40% ethyl acetate in hexane). Orange-yellow leaflets were obtained upon recrystallization from 95% ethanol, mp 202 °C. ^{1}H NMR ($CDCl_3$, 300 MHz): δ 8.05−7.95 (m, 4 H), 7.42−7.35 (m, 4 H), 7.30−7.25 (m, 2 H), 7.14 (dd, J = 8 Hz, 1 Hz, 2 H), 2.56 (s, 6000 H). ^{13}C NMR ($CDCl_3$, 90 MHz): δ 200.8, 145.3, 139.2, 137.0, 136.3, 128.2, 128.0, 124.8, 122.8, 121.3, 90.7, 36.7. EI-MS: m/z 354 (M^+, 100), 339 ($M^+ - CH_3$, 5), 325 ($M^+ - NCH_3$, 13), 297 ($M^+ - NCH_3 - CO$, 27). FTIR (KBr): 2980 (w), 2860 (w), 1743 (m), 1709 (s), 1590 (w), 1554 (w), 1500 (w), 1442 (m), 1315 (w), 1254 (m), 1190 (w), 1110 (w), 931 (m), 760 (m), 694 (w), 626 (w) cm^{-1}.

Synthesis of 4. The reaction was carried out using 0.21 g of 2-(methylamino)benzenethiol and an equimolar amount of ninhydrin. The pure compound was isolated in 65% yield after column chromatography (R_f = 0.35, 20% ethyl acetate in hexane). Recrystallization from 20% ethyl acetate in hexane gave red-brown needles, mp 206 °C. ^{1}H NMR ($CDCl_3$, 300 MHz): δ 8.09 (m, 2 H), 7.96 (m, 2 H), 7.10 (dt, J = 8, 1 Hz, 1 H), 6.95 (dd, J = 8, 1 Hz, 1 H), 6.73 (dt, J = 8, 1 Hz, 1 H), 6.45 (d, J = 8 Hz, 1 H), 2.78 (s, 3 H). ^{13}C NMR ($CDCl_3$, 90 MHz): δ 192.4, 147.5, 140.1, 136.9, 127.0, 124.6, 121.9, 121.1, 119.5, 107.4, 78.9, 31.7. EI-MS: m/z 281 (M^+, 57), 252 ($M^+ - NCH_3$, 7), 224 ($M^+ - NCH_3 - CO$, 100). FTIR ($CHCl_3$): 3072 (w), 3016 (m), 1758 (m), 1720 (s), 1600 (m), 1476 (m), 1349 (w), 1266 (w), 1237 (m), 1200 (w), 1161 (w), 1127 (w), 1025 (w), 949 (m), 782 (w), 761 (m), 737 (m), 674 (s), 627 (w) cm^{-1}.

Synthesis of 5. The reaction was carried out using 0.47 g of 8-(methylamino)-1-naphthalenethiol and an equimolar amount of ninhydrin. The pure compound (R_f = 0.72, 40% ethyl acetate in hexane) was isolated in 53% yield after column chromatography, using 20% ethyl acetate in hexane as the eluant. Upon recrystallization from 20% ethyl acetate in hexane, orange needles were obtained, mp 204 °C. ^{1}H NMR ($CDCl_3$, 300 MHz): δ 8.01−7.98 (m, 2 H), 7.92−7.89 (m, 2 H), 7.72 (dd, J = 8, 1 Hz, 1 H), 7.51 (t, J = 8 Hz, 1 H), 7.44 (dd, J = 8, 1 Hz, 1 H), 7.35 (t, J = 7 Hz, 1 H), 7.19 (dd, J = 7, 1 Hz, 1 H), 7.01 (dd, J = 8, 1 Hz, 1 H), 3.09 (s, 3 H). ^{13}C NMR ($CDCl_3$, 50 MHz): δ 192.4, 142.5, 138.7, 136.6, 133.9, 127.9, 127.1, 125.2, 124.4, 123.8, 123.5, 120.6, 120.3, 110.6, 68.1, 37.1. EI-MS: m/z 331 (M^+, 100), 316 ($M^+ - CH_3$, 6), 302 ($M^+ - NCH_3$, 6), 274 ($M^+ - NCH_3 - CO$, 92), 271 ($M^+ - CO - S$, 7), 256 ($M^+ - CO - S - CH_3$, 3). FTIR ($CHCl_3$): 3071 (w), 3026 (w), 1745 (w), 1713 (s), 1600 (w), 1568 (m), 1481 (w), 1458 (w), 1384 (w), 1349 (w), 1326 (w), 1261 (s), 1237 (w), 1190 (s), 1068 (w), 1021 (w), 972 (w), 820 (w), 809 (m), 786 (s), 756 (w), 730 (m), 676 (m), 662 (w), 629 (w) cm^{-1}.

(38) In some instances, in addition to condensation on C2 of the ninhydrin moiety, products of condensation on C1 were formed. The details on these spiro dyes will be published separately.

(39) Willets, A.; Rice, J. E.; Burland, D. M.; Shelton, D. P. *J. Chem. Phys.* **1992**, *97*, 7590.

Synthesis of 6. The reaction was carried out using 0.36 g of 1,8-bis(methylamino)naphthalene and an equimolar amount of 5,6-dimethoxyninhydrin. The pure compound ($R_f = 0.60$, 50% ethyl acetate in hexane) was isolated after column chromatography, using 40% ethyl acetate in hexane as the eluant, in 55% yield. Upon recrystallization from acetone, orange needles were obtained, mp 284 °C. ^{1}H NMR ($CDCl_3$, 300 MHz): δ 7.37 (s, 2 H), 7.35−7.27 (m, 4 H), 6.60 (dd, J = 7, 1 Hz, 2 H), 4.04 (s, 6 H), 2.80 (s, 6 H). ^{13}C NMR ($CDCl_3$, 50 MHz): δ 198.2, 157.1, 141.1, 135.9, 133.4, 126.7, 118.8, 113.2, 104.6, 103.1, 77.2, 56.9, 34.2. EI-MS: m/z 388 (M^+, 72), 373 ($M^+ - CH_3$, 3), 360 ($M^+ - CO$, 2), 359 ($M^+ - NCH_3$, 4), 331 ($M^+ - NCH_3 - CO$, 100), 316 ($M^+ - NCH_3 - CO - CH_3$, 9), 301 ($M^+ - NCH_3 - CO - 2CH_3$, 10). FTIR ($CHCl_3$): 3073 (w), 3002 (w), 2826 (w), 1739 (s), 1701 (s), 1627 (w), 1579 (s), 1504 (s), 1462 (m), 1418 (m), 1308 (s), 1148 (w), 1113 (s), 1000 (m), 919 (w), 876 (w), 834 (w), 793 (s), 784 (s), 738 (m), 650 (w) cm^{-1}.

Acknowledgment is made to the donors of the Petroleum Research Fund, administered by the American Chemical Society, for support of this research.

Supporting Information Available: Tables giving X-ray determined atomic coordinates, bond lengths, bond angles, and anisotropic displacement coefficients for **2**, **4**, **5**, and **6** (24 pages). This material is contained in many libraries on microfiche, immediately follows this article in the microfilm version of the journal, can be ordered from ACS, and can be downloaded from the Internet; see any current masthead page for ordering information and Internet access instructions.

JA9533003